# Magnetoelectricity in BiFeO_{3} films: First-principles-based computations and phenomenology

S. Prosandeev, Igor A. Kornev, and L. Bellaiche

Phys. Rev. B **83**, 020102 — Published 18 January 2011

DOI: 10.1103/PhysRevB.83.020102

# Magnetoelectricity in $BiFeO_3$ films: First-principles-based computations and phenomenology

S. Prosandeev[1*], Igor A. Kornev[2] and L. Bellaiche[1]
[1] *Physics Department, University of Arkansas, Fayetteville, Arkansas 72701, USA*
[2] *Laboratoire Structures, Propriétés et Modélisation des Solides, Ecole Centrale Paris, CNRS-UMR8580, Grande Voie des Vignes, 92295 Châtenay-Malabry Cedex, France*

A first-principles-based effective Hamiltonian is used to compute linear *and* quadratic magnetoelectric (ME) coefficients in epitaxial (001) $BiFeO_3$ thin films. Its predictions are analyzed within a phenomenological model that provides analytical expressions of the ME coefficients in terms of polarization, as well as, dielectric and magnetic susceptibilities. Main discoveries are: (i) the quadratic ME coefficient is dramatically enhanced by increasing the magnitude of the compressive strain within the Cc phase, as similar to the previously reported enhancement of the linear ME coefficient in these films; (ii) the enhancements of the linear and quadratic ME coefficients have the same macroscopic origin, namely an increase in the dielectric permittivity; and (iii) the relative contribution of *two* different free-energy terms on the total linear ME coefficient is extracted from the simulations. The analytical expressions also help in understanding other ME effects.

PACS numbers: 75.85.+t;77.55.Nv;77.80.B-



Multiferroics possess coupled ferroelectric and magnetic orders[1] and are currently receiving a lot of attention. These materials can exhibit a magnetoelectric (ME) coupling that allows electrical properties to be tuned by a magnetic field or, conversely, magnetic properties to be varied by an electric field. Several recent first-principles-based studies[2–5] have focused on *linear* ME coefficients to gain a better understanding of such coefficients and to find materials/effects leading to large ME couplings. In particular, it was found that enhanced linear ME responses can arise in highly-compressed epitaxial $BiFeO_3$ (BFO) thin films, as a result of structural softness[2]. Another kind of theory commonly used to study ME effects gathers phenomenological approaches[1,6–10]. These latter schemes are based on analytical expressions of the free energy, and typically only involve "straightforward" macroscopic quantities. They have the potential to be very useful to interpret in a simple manner experimental, as well as, first-principles data in multiferroics. For instance, they may reveal, in BFO films, (i) which precise macroscopic property leads to the reported optimization of the linear ME coefficient[2]; and (ii) which free-energy terms play a role in the linear ME coefficient. As a matter of fact, (at least) two *different* free energies can exist in multiferroics: one form that is proportional to a single product between magnetization, polarization and antiferromagnetic (AFM) vector[3,6,11] *versus* another free-energy term that involves a product between the square of the polarization and the square of the magnetization[12,13]. To the best of our knowledge, the relative contributions of these two free energies on the total linear ME coefficient of BFO is not known, despite the importance of this material.

Moreover, we are not aware of any direct first-principles calculation yielding *quadratic* ME coefficients in any multiferroic, while these coefficients are predominant over linear ME couplings in BFO systems[4,14–17]. It is thus presently unknown if these quadratic ME coefficients can also be dramatically enhanced by varying the epitaxial strain in BFO films, and, if so, what is the macroscopic reason behind it. Having a general analytical expression for the quadratic ME coefficients as a function of straightforward macroscopic properties may also help in better understanding magnetoelectricity in various multiferroics (including BFO).

The goal of this Rapid Communication is to provide answers to all the aforementioned issues. First-principles-based calculations reveal that the quadratic ME coefficient is also optimized in compressed BFO films. Furthermore, a phenomenological model used to analyze the *ab-initio* predictions (1) indicates that the previously reported enhancement of the linear ME coefficient[2] has the same macroscopic origin than the presently discovered optimization of the quadratic ME coupling, that is a strain-induced increase of the dielectric susceptibility; (2) reveals that two different free energies are indeed involved in the linear ME coefficient of BFO films; and (3) even allows to extract the relative contribution of these two free energies.

Here, we use the effective Hamiltonian approach of Ref. [4] to investigate (001) BFO films under compressive strain. Its degrees of freedom are: the local soft-mode distortions in every 5-atom unit cell $i$, $\mathbf{u}_i$ (which is directly proportional to the local electrical dipole of cell $i$); the homogeneous strain tensor, $\{\eta_H\}$[18]; inhomogeneous strain-related variables, $\mathbf{v}_i$[18]; the $\omega_i$ vectors whose directions are the axis about which the oxygen octahedron tilts in unit cell $i$, while their magnitudes provide the angle of such tilting[19]; and the $\mathbf{m}_i$ magnetic dipoles in the cells $i$[14]. All the parameters of this effective Hamiltonian scheme are extracted from first principles. As done in Refs. [2,20,21], the only distinction we assume between simulating a BFO bulk and an epitaxial (001) BFO film is that the latter is associated with the freezing of some components of the homogeneous strain tensor. More precisely, mechanical boundary conditions of

this film are mimicked by imposing that (in the basis for which the x-, y- and z-axis lie along the pseudo-cubic [100], [010] and [001] directions, respectively) $\eta_{H,xy}=\eta_{H,yx}=0$ and $\eta_{H,xx}=\eta_{H,yy}=\delta$, with $\delta$ being the value forcing the film to adopt the in-plane lattice constant of the substrate[22,23]. In practice, $\delta=(a_{\rm sub}-a_{\rm bulk})/a_{\rm bulk}$, where $a_{\rm sub}$ is the in-plane lattice parameter of the substrate and $a_{\rm bulk}$ is the 0 K pseudocubic lattice constant of bulk BFO. The total energy of the effective Hamiltonian scheme is then used in Monte-Carlo simulations, with up to $10^6$ sweeps. Note that first-principles-based effective Hamiltonians successfully reproduced important characteristics of bulk BFO, such as its structural ground state, quadratic magnetoelectric coefficients, and Néel and Curie temperatures[4,14,15]. The latest effective Hamiltonian developed for BFO[4] is also able to reproduce the spin-canting structure of $BiFeO_3$ films that generates a weak magnetization (of the order of $0.025\mu_B$) along with a strong G-type AFM vector[24].

Figures 1 show that this effective Hamiltonian approach predicts that up to a critical compressive misfit strain, $\delta_{crit}$, the ground state of epitaxial (001) films is a Cc phase that is characterized by: (1) by a polarization lying along $[uuv]$ directions, with the out-of-plane component of the polarization increasing when increasing the magnitude of the misfit compressive strain while the in-plane polarization adopts an opposite behavior; (2) oxygen octahedra tilting in antiphase about $[u'u'v']$ directions, with $v'$ (respectively, $u'$) increasing (respectively, decreasing) with the magnitude of $\delta$; (3) a G-type AFM vector that remains perpendicular to the polarization and to the axis about which the oxygen octahedra tilt for any compressive strain; and (4) a weak magnetization that rotates with $\delta$ (in order to stay orthogonal to both the AFM vector and the axis about which the oxygen octahedra tilt[4,25]). For compressive strains larger in magnitude than $\delta_{crit}$, the resulting ground state is characterized by (i) a strong out-of-plane polarization and (ii) and a large tetragonal axial ratio. Items (1)-(4) and (i)-(ii), as well as, the strain-induced energetic crossing between Cc and a strong ferroelectric phase, are all consistent with recent first-principles calculations[2,20,21]. On the other hand, the strong ferroelectric phase we predict at high compression has the tetragonal P4mm space group. As a result, it does not have any in-plane component of the polarization, unlike the monoclinic Cm state of Ref. [20]. It also does not exhibit any tilting of the oxygen octahedra, unlike the monoclinic Cc phase of Refs. [2,21]. However, all these first-principles calculations[2,20,21] found that the P4mm phase is quite close in energy to these Cm and Cc states, and that these latter monoclinic states both gradually transform into, and become, P4mm at high enough compressive strain (i.e., of the order of -6 or -7%)[26]. It is also interesting to realize that Fig. 1(a) indicates that the Cc state can survive for compressive strains larger in magnitude than $\delta_{crit}$[27]. This feature is in agreement with Refs. [2,20], and is relevant to our study because the linear ME coefficients of the Cc state were found to dramatically increase in the strain region for which this Cc phase is "only" metastable[2].

Figures 2(a) and 2(b) display the $\beta_{311}$ quadratic and $\alpha_{31}$ linear ME coefficients at 10K in the Cc phase, respectively, as predicted by our effective Hamiltonian approach – with the '1', '2' and '3' index corresponding to the pseudo-cubic [110], $[1\bar{1}0]$ and [001] directions, respectively[28]. These coefficients are calculated by fitting the polarization-versus-magnetic field curve by a polynomial of degree 2 for any $\delta$ and up to a field of 100 Tesla[4,14,15]. Figure 2(b) confirms a finding of Ref. [2], namely that increasing the magnitude of $\delta$ within the Cc state leads to a spectacular enhancement of the magnitude of the linear ME coefficient (note that our predicted magnitude of this coefficient is equal or larger than $5ps/m$ for $\delta$ larger in magnitude than 5%, which agrees very well with the first-principles results of Ref. [2]). Interestingly, Fig. 2(a) reveals that the $\beta_{311}$ quadratic coefficient also *considerably increases in magnitude at the same time* (note that we predict a magnitude of $0.3\times10^{-19}$ s/A for $\beta_{311}$ at zero strain, which is precisely the low-temperature experimental value of BFO bulk[16]).

Let us now analyze the results of Figs. 2 via a general phenomenological model. For that, we first start with the definition of the $\alpha_{ij}$ linear and $\beta_{ijk}$ quadratic ME coefficients[12]:

$$\alpha_{ij}=\frac{\partial P_i}{\partial H_j}=-\frac{\partial^2\Phi}{\partial E_i\partial H_j}\quad and\quad \beta_{ijk}=\frac{\partial^2 P_i}{\partial H_j\partial H_k}=-\frac{\partial^3\Phi}{\partial E_i\partial H_j\partial H_k}\quad , \tag{1}$$

where $\Phi$ is the free energy. $P_i$ and $E_i$ are the i-component of the polarization and of the electric field, respectively. $H_j$ represents the j-component of the magnetic field. The next step is to determine the terms of the free energy that do not vanish in the derivations of Eqs.(1). To the lowest orders, such energetic terms are two-fold and are[12]:

$$\Phi^{(1)}=\sum_{pq}\lambda_{pq}P_pP_pM_qM_q\quad and\quad \Phi^{(2)}=\sum_{pqr}g_{pqr}M_pL_qP_r\quad , \tag{2}$$

where the sums run over the components of the magnetization ($M$), AFM vector ($L$) and polarization. $\lambda_{pq}$ and $g_{pqr}$ are two-rank and third-rank tensors, respectively, that depend on the symmetry of the crystal and are material's dependent. It is straightforward to demonstrate that inserting Eqs.(2) into Eqs.(1) gives:

$$\alpha_{ij}=\alpha_{ij}^{(1)}+\alpha_{ij}^{(2)}\quad with\quad \alpha_{ij}^{(1)}=-4\varepsilon_0\textstyle\sum_{pq}\lambda_{pq}P_p\chi^P_{pi}M_q\chi^M_{qj}\quad and\quad \alpha_{ij}^{(2)}=-\sum_{pqr}g_{pqr}\chi^P_{ri}L_q\chi^M_{pj},$$

$$and \quad \beta_{ijk} = \beta^{(2)}_{ijk} = -4\varepsilon_0 \sum_{pq} \lambda_{pq} P_p \chi^P_{pi} \chi^M_{qj} \chi^M_{qk} \quad , \tag{3}$$

where the (1) and (2) superscripts indicate that the corresponding coefficients originate from the $\Phi^{(1)}$ and $\Phi^{(2)}$ free energies, respectively. $\varepsilon_0$ is the dielectric permittivity of vacuum, and $\chi^P$ represents the dielectric susceptibility tensor (that is, $\chi^P_{pi} = \frac{1}{\varepsilon_0}\frac{\partial P_p}{\partial E_i}$). Finally, $\chi^M_{qj}$ are the elements of the magnetic susceptibility tensor, i.e. $\chi^M_{qj} = \frac{\partial M_q}{\partial H_j}$.

Interestingly, our effective Hamiltonian approach predicts that, in the studied BFO film, $\chi^P_{33}$ and $\chi^M_{11}$ are the largest elements of the dielectric and magnetic susceptibility tensor, respectively (such quantities are displayed in Fig. 2(c) and 2(d)). As a result, one can rewrite Eqs. (3) for the ME coefficients shown in Figs. 2(a) and 2(b) as:

$$\beta_{311} = \beta^{(2)}_{311} = -4\varepsilon_0 \lambda_{31} P_3 \chi^P_{33} \chi^M_{11} \chi^M_{11} \quad , \tag{4}$$

and

$$\alpha_{31} = \alpha^{(1)}_{31} + \alpha^{(2)}_{31} \quad with \quad \alpha^{(1)}_{31} = -4\varepsilon_0 \lambda_{31} P_3 \chi^P_{33} M_1 \chi^M_{11} \quad and \quad \alpha^{(2)}_{31} = -g_{123} \chi^P_{33} L_2 \chi^M_{11}. \tag{5}$$

Figure 2(a) shows that one can indeed fit very well the computed $\beta_{311}$ by Eq. (4) with a strain-independent $\lambda_{31}$ coefficient equal to $4.8 \times 10^{-3}$ SI. This equation, along with Figs. 1(b), 2(c) and 2(d), allow to prove that the increase of the quadratic ME coefficient with strain is mostly due to the gain in the dielectric permittivity, when going towards the boundary of the stability of the Cc phase. Interestingly and as revealed by Fig. 2(b), $\alpha^{(1)}_{31} = -4\varepsilon_0 \lambda_{31} P_3 \chi^P_{33} M_1 \chi^M_{11}$ (using the $\lambda_{31}$ coefficient extracted from the fit of $\beta_{311}$) significantly differs from the computed $\alpha_{31}$ linear coefficient. As a matter of fact and as indicated in Fig. 2(b), one needs to also incorporate the second part of the linear ME coefficient (i.e., $\alpha^{(2)}_{31} = -g_{123} \chi^P_{33} L_2 \chi^M_{11}$, with a fixed, misfit-independent $g_{123}$ coefficient equal to $0.6 \times 10^{-4}$ SI) to precisely reproduce the computed linear ME coefficient. Such finding reveals that the two free energies of Eqs.(2) are both playing a role on the magnitude of the total linear ME coefficient of BFO. These two terms should thus be both accounted for when studying ME couplings in BFO films[13]. Moreover, looking at the behavior of the properties depicted in Figs. 1(b), 1(d), 1(e), 2(c) and 2(d) – and that are involved in the analytical expression of Eq. (5) – reveals that the enhancement of the linear ME coefficient when increasing the magnitude of the misfit strain mostly originates from the sudden increase of the dielectric susceptibility too[29].

Interestingly, Eqs. (3) are applicable to *any* multiferroic and are very informative. For instance, one can immediately realize that the quadratic ME coefficients "only" require the structural phase to be polar, and therefore do not need the phase to be magnetically-ordered, in order to exist. On the other hand, Eqs.(3) tell us that having non-vanishing linear coefficients is only possible in structural states that are magnetically-ordered. The linear ME coefficient reduces to $\alpha^{(1)}_{ij}$ for ferromagnetic systems, while an AFM order leaves only $\alpha^{(2)}_{ij}$ as the non-zero contribution to the total $\alpha_{ij}$ coefficient. Eqs (3) also reveal that $\alpha^{(1)}_{ij}$ and $\alpha^{(2)}_{ij}$ are both "activated" in spin-canted magnetic structures in which a weak ferromagnetism coexists with a strong AFM vector (exactly as in BFO films below $\simeq$ 640K[24]). In contrast, cycloidal magnetic structures that result in the annihilation of the macroscopic magnetization and AFM vector can not have any linear ME coefficients according to Eqs.(3) – as consistent with the case of BFO bulk[17]. The rather simple expressions of Eqs (3) also indicate the "recipes" to follow to have strong ME coefficients. In particular, large values of the dielectric and magnetic susceptibilities are automatically associated with large quadratic ME coefficients, assuming a non-zero polarization. As a result, finding systems simultaneously possessing just above 300K *a second-order ferromagnetic transition and a second-order ferroelectric transition* is the ideal choice to generate huge $\beta_{ijk}$ coefficients at room temperature. Similarly, the expression of $\alpha^{(2)}_{ij}$ implies that an antiferromagnet will have a large linear ME coefficient for temperatures below the Néel temperature for large values of the *dielectric* susceptibility. A second-order or even tricritical ferroelectric transition occurring in an AFM phase will thus generate giant linear ME effects. It is likely that Eqs. (3) that express linear and quadratic ME coefficients can further help in understanding other magnetoelectric effects[30] and can serve as a guide to find desired materials with optimal magnetoelectric response.

This work is supported by ONR Grants N00014-08-1-0915 and N00014-07-1-0825, DOE grant DE-SC0002220, and NSF grants DMR-0701558 and DMR-0080054. Some computations were made possible thanks to the MRI NSF grant 0722625. S.P. appreciates grant 08-02-92006NNSa from RFBR.

*also Southern Federal University, 344090 Rostov on Don, RUSSIA.

[1] G.A. Smolenskii and I.E. Chupis, *Sov. Phys. Usp.* **25**, 475 (1982).

[2] J. C. Wojdel and J. Íñiguez, Phys. Rev. Lett. **105**, 037208 (2010).
[3] M. Mostovoy, A. Scaramucci, N. A. Spaldin, and K. T. Delaney, Phys. Rev. Lett. **105**, 087202 (2010).
[4] D. Albrecht *et al*, Phys. Rev. B **81**, 140401(R) (2010).
[5] K. T. Delaney, E. Bousquet, N. A. Spaldin, arXiv:0912.1335v2.
[6] G. T. Rado, Phys. Rev. **128**, 2546 (1962).
[7] I. E. Chupis, Low Temp. Phys. **31**, 858 (2005).
[8] M. I. Bichurin and V. M. Petrov, Soviet Physics - Solid State, **29**, 1445 (1987).
[9] D. A. Filippov, G. Srinivasan and A. Gupta, J. Phys.: Condens. Matter **20**, 425206 (2008).
[10] E. A. Eliseev *et al*, Phys. Rev. B **82**, 085408 (2010).
[11] I. Kornev *et al*, Phys. Rev. B **62**, 12247 (2000).
[12] L. D. Landau and E. M. Lifshitz, Electrodynamics of continuous media, Pergamon, Oxford, 1960.
[13] M. Daraktchiev, G. Catalan, and J. F. Scott, Phys. Rev. B **81**, 224118 (2010).
[14] I. Kornev *et al*, Phys. Rev. Lett. **99**, 227602 (2007).
[15] S. Lisenkov, I. A. Kornev, and L. Bellaiche, Phys. Rev. B **79**, 012101 (2009).
[16] C. Tabares-Munoz *et al*, Jap. Journ. Appl. Phys. **24**, 1051 (1985).
[17] G. Catalan and J. F. Scott, Adv. Mater. 21, 2463 (2009).
[18] W. Zhong, D. Vanderbilt and K. M. Rabe, Phys. Rev. Lett. **73**, 1861 (1994); Phys. Rev. B **52**, 6301 (1995).
[19] I. Kornev *et al*, Phys. Rev. Lett. **97**, 157601 (2006).
[20] B. Dupé *et al*, Phys. Rev. B 81, 144128 (2010).
[21] A. J. Hatt, N. A. Spaldin, and C. Ederer, Phys. Rev. B 81, 054109 (2010).
[22] I. Kornev, H. Fu and L. Bellaiche, Phys. Rev. Lett. **93**, 196104 (2004).
[23] N.A. Pertsev, V. G. Kukhar, H. Kohlstedt, and R. Waser, Phys. Rev. B **67**, 054107 (2003).
[24] H. Bea *et al*, *Appl. Phys. Lett.* **87**, 072508 (2005); H. Bea *et al*, *Philos. Mag. Lett.* **87**, 165 (2007).
[25] C. Ederer and N.A. Spaldin, *Phys. Rev. B* **71**, 060401 (2005).
[26] The presently used effective Hamiltonian approach does not predict a Cm state, but rather a P4mm phase, likely because of the omission of some subtle energetic terms. Note also that we predict that the P4mm state has an AFM vector aligned along the [1-10] direction (not shown here) but does not exhibit any magnetization (due the lack of oxygen octahedra tilting[4,25]).
[27] Our effective Hamiltonian yields $\delta_{crit} \simeq$ -6% , which is in good agreement with the value of -5.5% reported in Ref. [20]. It is slightly larger in magnitude than the values of -4.5% predicted in Refs. [2,21]. Such variation between different calculations is due to the high sensitivity of $\delta_{crit}$ with technical details of first-principles[20]). Similarly, we found that slightly varying one specific parameter of the effective Hamiltonian approach results in a rather strong variation of $\delta_{crit}$.
[28] $\beta_{311}$ is defined as $\frac{\partial^2 P_3}{\partial H_1 \partial H_1}$, and $\alpha_{31}$ is defined as $\frac{\partial P_3}{\partial H_1}$, where $P_3$ is the component of the polarization along the '3' axis while $H_1$ is the component of the magnetic field along the '1' axis.
[29] Note that the so-called structural softness of Ref. [2] (that was found to be the microscopic origin behind the large values of the linear ME coefficient in highly compressed BFO films) is consistent with the sudden increase of the dielectric susceptibility reported here.
[30] For instance, Eqs. (3) can be used to understand a recent first-principles finding, namely that the *electronic* contribution of the linear ME coefficient in (AFM) $Cr_2O_3$ can *not* be neglected with respect to its *ionic* contribution[5]. As a matter of fact, one can assume by looking at $\alpha_{ij}^{(2)}$ of Eqs. (3) that the *electronic* contribution of the linear ME coefficient mostly originates from the electronic part of the dielectric susceptibility (to be denoted by $\chi_{el}^P$) while its ionic contribution involves the ionic part of the dielectric susceptibility (to be denoted by $\chi_{ion}^P$). In other words, one can re-writte the $\alpha_{ij}^{(2)}$ of Eqs. (3) as $-\sum_{pqr} g_{pqr} \chi_{el,ri}^P L_q \chi_{pj}^M - \sum_{pqr} g_{pqr} \chi_{ion,ri}^P L_q \chi_{pj}^M$, where the first sum is the electronic linear ME coefficient while the second sum characterizes the ionic linear ME coefficient. Performing first-principles calculations on $Cr_2O_3$ shows that $\chi_{el}^P$ is of the same order than $\chi_{ion}^P$. This explains why both the electronic and ionic part of the linear ME coefficient should be taken into account to compute the low-temperature total linear ME coefficient in this material. Note also that Eqs. (1) indicate that the quadratic ME coefficients correspond to the derivative of the magnetic susceptibility with respect to the electric field. One can also define *another* ME coefficient as $-\frac{\partial^3 \Phi}{\partial H_i \partial E_j \partial E_k} = \frac{\partial^2 M_i}{\partial E_j \partial E_k} = \varepsilon_0 \frac{\partial \chi_{jk}^P}{\partial H_i}$.

FIGURE CAPTIONS

FIG.1 (color online). Predicted properties of epitaxial (001) BFO films at 10K in the Cc (filled symbols) and P4mm (open symbols) structural phases, as a function of the misfit strain: the total internal energy per 5 atoms (Panel (a)), averaged local soft-mode – which is proportional to the electrical polarization – (Panel (b)), average antiphase tilting angle of oxygen octahedra (Panel (c)), G-type antiferromagnetic vector (Panel (d)), magnetization (Panel (e)), and tetragonal axial ratio (Panel (f)). The x-, y- and z-axes are chosen along the pseudo-cubic [100], [010] and [001] directions respectively. The tilting of oxygen octahedra and the magnetization are both found to vanish in the P4mm state, while the G-type AFM vector is along the $[1\bar{1}0]$ pseudo-cubic direction.

FIG.2. Other predicted properties of epitaxial (001) BFO films at 10K in the Cc state, as a function of the misfit strain: the $\beta_{311}$ quadratic magnetoelectric coefficient (Panel (a)), $\alpha_{31}$ linear ME element (Panel (b)), $\chi_{33}^{P}$ dielectric susceptibility (Panel (c)), and $\chi_{11}^{M}$ magnetic susceptibility (Panel (d)). The dashed line in Panel (a) corresponds to the fit of the data by Eq. (4). The solid line in Panel (b) represents the fitting by Eq. (5), while the dashed line shows the fitting by the sole $\alpha_{31}^{(1)}$ of Eq. (5). The '1', '2' and '3' subscripts are associated with the pseudo-cubic [110], $[1\bar{1}0]$ and [001] directions, respectively.

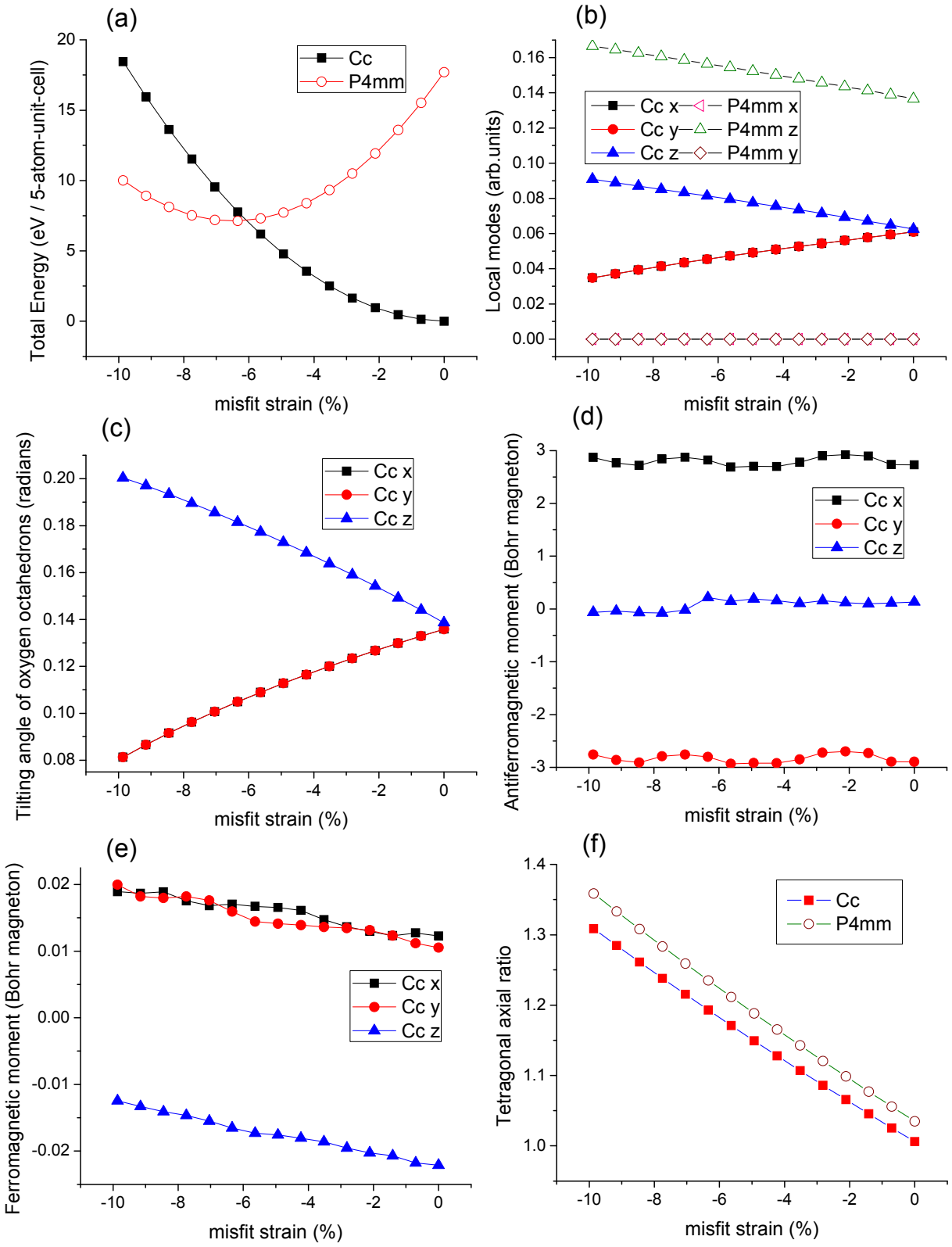


Figure 1 LX12190BR 08Dec2010

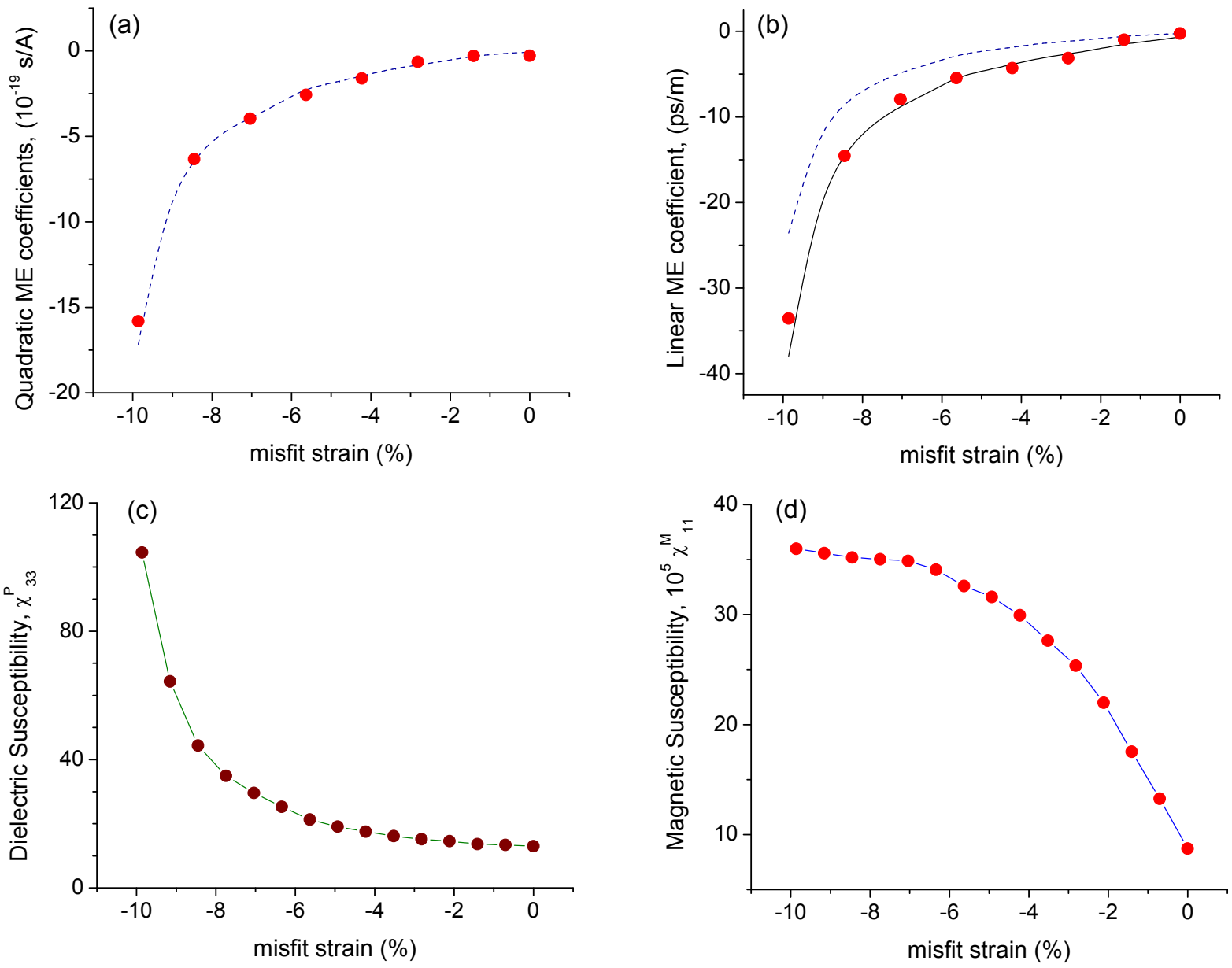


Figure 2 LX12190BR 08Dec2010